Hybrid Tracking Control of Eye-in-Hand Robotic Manipulators

Wen-Chung Chang and Chih-Wei Cho
Department of Electrical Engineering
National Taipei University of Technology
Taipei 106, Taiwan, R.O.C.

Abstract

Classical force and vision-based tracking control approaches typically require expensive six-axis force sensors in addition to vision sensors. In this article, a new approach is presented which only requires a single-axis force senor together with a laser cross projector in addition to a vision sensor. The key idea is to estimate the direction normal to an unknown 3-D surface by projecting and reconstructing a laser cross on it. The proposed autonomous task is to drive the end-effector of a 6-DOF manipulator to a visually determined trajectory and continue tracking the trajectory in desired pose, contact force, and speed. The proposed hybrid force and vision-based control approach is successfully validated in a real task environment by performing experiments with an industrial robotic manipulator on an arbitrary-shaped acrylic fiber 3-D object.

1 Introduction

Vision is becoming a popular sensor in robot control since it can extract extensive information without contacting with the environment. Based on available visual information, appropriate feedback lows can be synthesized for variety of control applications [1, 2]. Xiao *et al.* [3], proposed force and position control of a robotic manipulator in Cartesian space with an expensive 6-axis force sensor and a CCD video camera. In [4], an autonomous dexterous planar robotic system capable of tracking unknown contours has been presented and validated in experiments. This system can guarantee task precision employing only a single-axis force sensor and an imprecisely calibrated CCD camera. In this research, force and pose tracking control can be further performed on 3-D unknown surfaces by a low-cost single-axis force sensor, a CCD camera, and a laser cross projector. In order to control the pose of the end-effector with respect to an unknown 3-D surface, the direction normal to the tangential plane at the contacting point, a normal vector, must be estimated. This normal vector is computed based on the reconstruction of the projected laser cross onto the unknown surface provided that the fixed transformation between the coordinate systems of the camera and the laser projector is known a priori.

The configuration of the proposed autonomous system is shown in Figure 1, where the system includes a robot arm, an unknown surface, a laser cross projector, a PC, and a CCD camera. The problem of in-

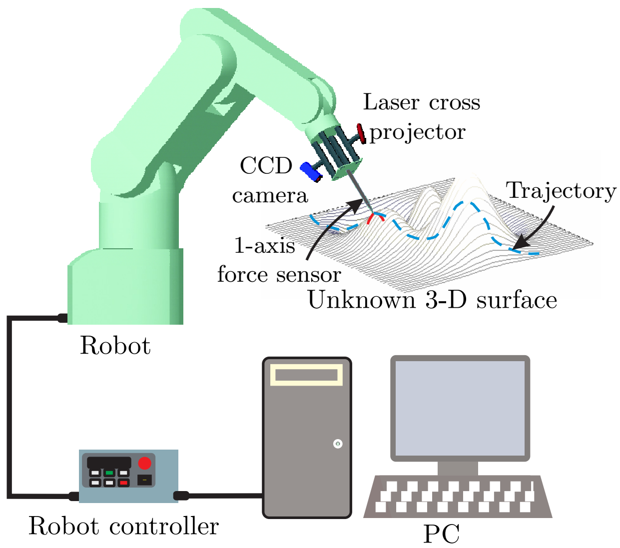

Figure 1: System configuration.

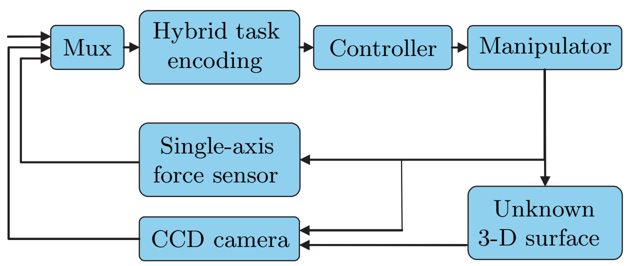

Figure 2: Hybrid control structure.

terest is to simultaneously control the normal contact force and the pose of a six-degree-of-freedom robotic manipulator on the unknown 3-D surface. The goal of the autonomous task is to drive the end-effector to the trajectory and continue tracking the trajectory in desired pose and contact force. The proposed hybrid control structure is illustrated in Figure 2.

2 Normal vectors on 3-D surface

2.1 Detection of laser cross

As the color of the laser cross is different from the surrounding environment, the laser cross could be detected by color filtering and connected components labelling [5]. A typical observed image from a CCD camera and the corresponding image processing results can be seen in Figure 3. In order to locate the two curves

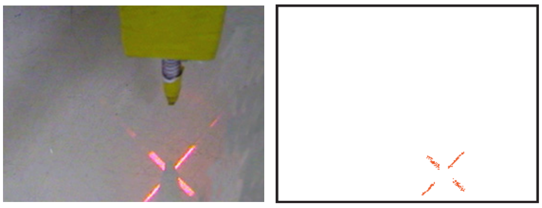

Figure 3: Laser cross on image plane.

that the laser cross is composed of, one could first identify the corresponding two sets of pixels and apply least square algorithm to determine their equations in image space. An effective way of computing the center of the cross for correctly allocating sets of pixels to the two curves is as follows. Let $[\ u \quad v\ ]^T$ be the 2-D coordinates in the image plane, α denote the distance between the edges of laser cross at fixed u, and β denote the distance between the edges of laser cross at fixed v as illustrated in Figure 4. By determining the

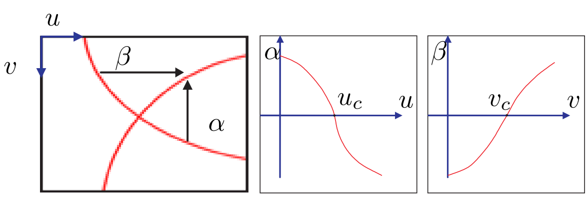

Figure 4: Laser cross curves on image plane{*left*}, $u\alpha$-plane{*middle*}, and $v\beta$-plane{*right*}.

equation of the curves

$$\alpha = g_1(u) \text{ and } \beta = g_2(v) \tag{1}$$

on the $u\alpha$-plane and the $v\beta$-plane as illustrated in Figure 4, the image coordinate of the laser cross center $[\ u_c \quad v_c\ ]^T$ are calculated by setting $\alpha = 0$ and $\beta = 0$ in (1). To determine the two curves and the precise center of laser cross, four regions are partitioned by the previously detected laser cross center $[\ u_c \quad v_c\ ]^T$. The curve in quadrant I and quadrant III can be estimated by least square algorithm. Similarly, the other curve in quadrant II and quadrant IV can also be estimated.

2.2 Reconstruction of normal vectors

To determine the directional vector normal to the 3D unknown surface, the image projection of laser cross onto the unknown surface is used to estimate the normal vector. Firstly, calculate the transformation matrix between the camera and the laser projector, and then the transformation matrix between the laser projector and the robot. Finally, reconstruct the projected laser cross on the surface in laser projector frame by the known transformation between the camera and the laser projector as shown in Figure 5. Specifically, when projecting a laser line to form the yz-plane in the laser projector frame, one can reconstruct a 3-D laser point $\bar{\boldsymbol{m}}$ with ${}^I\bar{\boldsymbol{m}}$ as the 3-D coordinate of its projection on the image space by setting the x-component of $\bar{\boldsymbol{m}}$ to be zero in the following equality.

$$\bar{\boldsymbol{m}} - \boldsymbol{c} = k({}^I\bar{\boldsymbol{m}} - \boldsymbol{c}) \tag{2}$$

Similarly, one can reconstruct a 3-D laser point by setting the y-component of $\bar{\boldsymbol{m}}$ to be zero in (2) if a laser line is projected to form the xz-plane. Based on

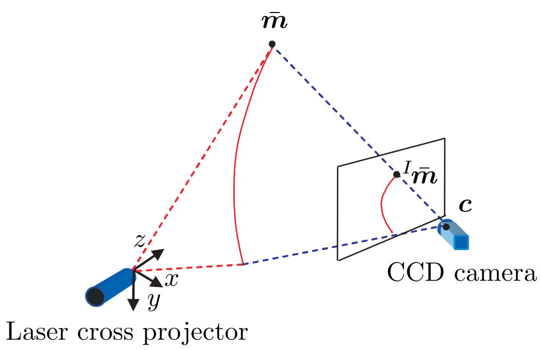

Figure 5: Reconstruction of laser cross curves.

the reconstructed laser cross in Cartesian space, one can compute the normal vector $\boldsymbol{n}$ at the laser cross center, which is the cross product of the two tangential lines at the laser cross center.

3 Hybrid control design

There are three subtasks for the hybrid task including position, orientation, and force control tasks.

3.1 Position control

The purpose of this subtask is to control the robot to reach the desired target position. The task can be divided into two parts. The first part is an image-based set-point control task. The second part is a contacting control task. Based on the perspective projective model G of the camera, the image coordinate ${}^{I}\boldsymbol{r}$ of a point feature $\boldsymbol{r} \in \Re^3$ can be computed as

$$ {}^{I}\boldsymbol{r} = G(\boldsymbol{r}) = \begin{bmatrix} \gamma \frac{\boldsymbol{i}^T(\boldsymbol{r}-\boldsymbol{c})}{\boldsymbol{k}^T(\boldsymbol{r}-\boldsymbol{c})} \\ \gamma \frac{\boldsymbol{j}^T(\boldsymbol{r}-\boldsymbol{c})}{\boldsymbol{k}^T(\boldsymbol{r}-\boldsymbol{c})} \end{bmatrix} \tag{3} $$

where γ is the focal length and $\boldsymbol{c}$ is the optical center of the camera, and $\boldsymbol{i}^T$, $\boldsymbol{j}^T$, and $\boldsymbol{k}^T$ are the row vectors of the rotation matrix from the base frame to the camera frame. The encoded error for this task can be defined as

$$ \boldsymbol{e}_1 = {}^{I}\boldsymbol{r} - {}^{I}\boldsymbol{r}^* \tag{4} $$

where $\boldsymbol{r}$ and $\boldsymbol{r}^*$ are the positions of the end-effector tip and the laser cross center respectively. Differentiate (4) with respect to time, it follows that

$$ \dot{\boldsymbol{e}}_1 = \boldsymbol{J}_1(\boldsymbol{r})\dot{\boldsymbol{r}} \tag{5} $$

where

$$ \boldsymbol{J}_1(\boldsymbol{r}) = \begin{bmatrix} \frac{f}{\boldsymbol{k}^T(\boldsymbol{r}-\boldsymbol{c})} \left(\boldsymbol{i}^T - \frac{\boldsymbol{i}^T(\boldsymbol{r}-\boldsymbol{c})}{\boldsymbol{k}^T(\boldsymbol{r}-\boldsymbol{c})} \boldsymbol{k}^T \right) \\ \frac{f}{\boldsymbol{k}^T(\boldsymbol{r}-\boldsymbol{c})} \left(\boldsymbol{j}^T - \frac{\boldsymbol{j}^T(\boldsymbol{r}-\boldsymbol{c})}{\boldsymbol{k}^T(\boldsymbol{r}-\boldsymbol{c})} \boldsymbol{k}^T \right) \end{bmatrix} \tag{6} $$

The image-based position control law capable of driving $\boldsymbol{e}_1$ to zero can be chosen as follows.

$$ \dot{\boldsymbol{r}} = -\left(\boldsymbol{J}_1 \circ \boldsymbol{L}(\boldsymbol{\theta}) \right)^+ \boldsymbol{e}_1 \tag{7} $$

where $\boldsymbol{L}$ denotes the forward kinematic function and the superscript $+$ denotes the pseudo-inverse. Since one cannot perform 3D positioning task with only single-camera vision, a contacting control law is considered which together with the image-based feedback law can guarantee precise positioning at the target point $\boldsymbol{r}^*$ on the 3-D trajectory. Let $\boldsymbol{P} \in \Re^{3\times 3}$, the projector onto the null space of $\boldsymbol{J}_1$, be defined as

$$ \boldsymbol{P} = \boldsymbol{I} - \boldsymbol{J}_1^+ \boldsymbol{J}_1. \tag{8} $$

Consider the feedback connection $\dot{\boldsymbol{r}} = \dot{\boldsymbol{r}}_p$, where

$$ \dot{\boldsymbol{r}}_p = -\left(\boldsymbol{J}_1 \circ \boldsymbol{L}(\boldsymbol{\theta}) \right)^+ \boldsymbol{e}_1 + k_1(f)\boldsymbol{P}\boldsymbol{l} \tag{9} $$

$\boldsymbol{l} = {}^{I}\bar{\boldsymbol{r}}^* - \boldsymbol{c}$, f denotes the contact force, and with suitably defined positive numbers k_1 and δ

$$ k_1(f) = \begin{cases} 0 & f > \delta; \text{if contacting} \\ k_1 & f \leq \delta; \text{otherwise} \end{cases} . \tag{10} $$

In the light of (5) and (9), it follows that

$$ \dot{\boldsymbol{e}}_1 = -\boldsymbol{e}_1. \tag{11} $$

Therefore, the end-effector tip continues reaching the laser cross center while $\boldsymbol{e}_1 \to 0$ exponentially.

3.2 Orientation control

Based on the reconstructed normal vector $\boldsymbol{n}$ and the orientation of the end-effector, denoted by $\boldsymbol{z}$, one can define the encoded error for the orientation control subtask as

$$ \boldsymbol{e}_2 = \boldsymbol{z}(\boldsymbol{\theta}) \times \boldsymbol{n} = \boldsymbol{h}(\boldsymbol{\theta}) \tag{12} $$

where $\boldsymbol{\theta}$ denotes the joint position vector and $\boldsymbol{z}$ can be computed based the forward kinematics of the manipulator. Differentiate (12) with respect to time, it follows that

$$ \dot{\boldsymbol{e}}_2 = \frac{\partial \boldsymbol{h}(\boldsymbol{\theta})}{\partial \boldsymbol{\theta}} \dot{\boldsymbol{\theta}} = \boldsymbol{J}_2(\boldsymbol{\theta})\dot{\boldsymbol{\theta}} \tag{13} $$

The following joint control law when placed in the feedback loop, $\dot{\boldsymbol{\theta}} = \dot{\boldsymbol{\theta}}_o$, is capable of driving $\boldsymbol{z}$ to align with $\boldsymbol{n}$.

$$ \dot{\boldsymbol{\theta}}_o = -\boldsymbol{J}_2(\boldsymbol{\theta})^+ \boldsymbol{e}_2 \tag{14} $$

3.3 Force control

This subtask is to maintain the required contact force along the normal direction to the unknown surface. Let f_d denote the desired contact force and the force encoded error be defined as

$$ e_f = f - f_d. \tag{15} $$

Consider the feedback connection $\dot{\boldsymbol{r}} = \dot{\boldsymbol{r}}_f$, where

$$ \dot{\boldsymbol{r}}_f = k_f e_f \boldsymbol{n}, \; k_f > 0. \tag{16} $$

Then, the joint velocity command for the force control task can be synthesized as follows.

$$ \dot{\boldsymbol{\theta}}_f = \boldsymbol{J}_m(\boldsymbol{\theta})^{-1} \begin{bmatrix} \dot{\boldsymbol{r}}_f \\ 0_{3\times 1} \end{bmatrix} \tag{17} $$

where $\boldsymbol{J}_m(\boldsymbol{\theta}) \in \Re^{6\times 6}$ is the mechanical Jacobian of the manipulator.

3.4 Hybrid control

The encoded error for the pose control task can thus be defined as

$$\boldsymbol{e} = \begin{bmatrix} \boldsymbol{e}_1 \\ \boldsymbol{e}_2 \end{bmatrix} \tag{18}$$

Differentiate (18) with respect to time, it follow that

$$\dot{e} = \boldsymbol{M}(\boldsymbol{\theta})\dot{\boldsymbol{\theta}} \tag{19}$$

where

$$\boldsymbol{M}(\boldsymbol{\theta}) = \begin{bmatrix} (\boldsymbol{J}_1 \circ \boldsymbol{L}(\boldsymbol{\theta}))\,\boldsymbol{J}_{m1}(\boldsymbol{\theta}) \\ \boldsymbol{J}_2(\boldsymbol{\theta}) \end{bmatrix}; \boldsymbol{J}_{m1}(\boldsymbol{\theta}) = \frac{\partial \boldsymbol{L}(\boldsymbol{\theta})}{\partial \boldsymbol{\theta}}.$$

With the understanding that the force control law does not disturb the pose control law, the hybrid control law in the joint space capable of driving $\boldsymbol{e}$ and e_f to zero exponentially can thus be defined as follows.

$$\dot{\boldsymbol{\theta}} = -\boldsymbol{M}^{+}(\boldsymbol{\theta})\boldsymbol{e} + \dot{\boldsymbol{\theta}}_f \tag{20}$$

4 Experiments

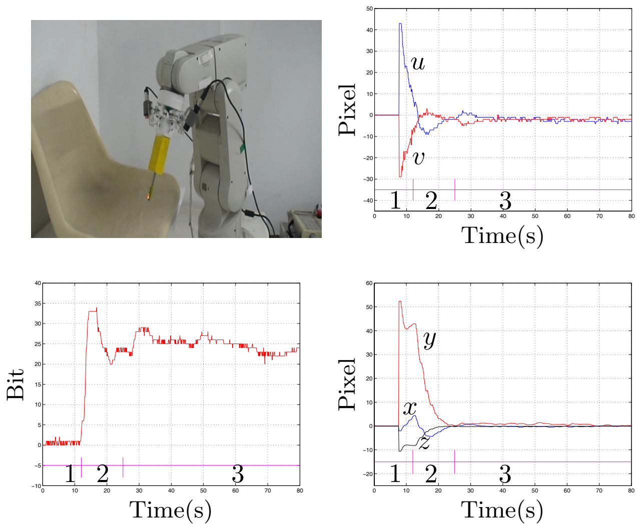

Figure 6: Experimental setup{*top left*}, position tracking error{*top right*}, force tracking error{*bottom left*}, and orientation tracking error{*bottom right*} .

The experimental system is composed of a 6-DOF Mitsubishi robot RV-1A, a JAI CV-S3200 camera, a laser cross projector, a P4-2.4G computer, and an arbitrary-shaped acrylic fiber 3-D object as illustrated in Figure 6. Successive stages in the autonomous hybrid tracking control are as follows. In Stage 1, the tool tip is driven to the laser cross center with orientation normal to the unknown surface by employing the proposed pose control law. In Stage 2, force control is applied while maintaining the desired pose. In Stage 3, the tool is controlled to follow the moving laser cross in desired pose and contact force. The tracking errors for position, orientation, and force in these stages are shown in Figure 6. In these experiments, the proposed hybrid control approach has demonstrated satisfactory performance on tracking control.

5 Conclusion

This paper presents a seemingly novel approach to autonomously control the pose of a robotic manipulator with respect to an unknown 3-D surface. In particular, the end-effector can be driven to a set-point and trajectory on the surface while kept normal to the surface. A low-cost single-axis force sensor together with a CCD camera and a laser cross projector are required to perform such control tasks. Compared with existing approaches, the proposed system is not only effective but also less expensive.

Acknowledgements

This research is supported by the National Science Council of Taiwan, R.O.C. under grants NSC 94-2213-E-027-006 and NSC 95-2221-E-027-049.

References

[1] Gregory D. Hager and Wen-Chung Chang and A. Stephen Morse, "Robot hand-eye coordination based on stereo vision," *IEEE Control Syst. Mag.*,Vol. 15, pp. 30-39, 1995.

[2] Seth A. Hutchinson and Gregory D. Hager and Peter I. Corke, "A Tutorial on Visual Servo Control," *IEEE Trans. Robot. Automat.*,Vol. 12, pp. 651-670, 1996.

[3] Di Xiao and B.K. Ghosh and Ning Xi and T. J. Tarn, "Sensor-Based Hybrid Position/Force Control of a Robot Manipulator in an Uncalibrated Environment," *IEEE Transactions on Control Systems Technology*,Vol. 8, pp. 635-645, 2000.

[4] Wen-Chung Chang, "Hybrid Force and Vision-Based Contour Following of Planar Robots," *Journal of Intelligent and Robotic Systems*,Vol. 47, pp. 215-237, 2006.

[5] I. Pitas, *Digital Image Processing Algorithms and Applications*, Wiley, 2000.